Local Structure of Atactic Polystyrene Investigated by Molecular Dynamics Method

ANDREI V. KOMOLKIN, SERGEY G. POLUSHIN, VYACHESLAV B. ROGOZHIN,
ALEXANDRA A. LEZOVA, GALINA E. POLUSHINA, IRINA A. SILANTEVA
Department of Physics,
Saint Petersburg State University,
Saint Petersburg, 199034,
RUSSIAN FEDERATION

Abstract: Molecular dynamics computer simulation of three substances ethylbenzene (EB), pentastyrene (PS-5), and polystyrene-25 (PS-25) was performed to investigate the local order of the phenyl rings in monomers and side-chain polymers. Monomer molecules (EB) tend to be in T-configuration, which corresponds to isotropic local structure. Phenyl rings in chained molecules PS-5 and PS-25 partly cooperate in both parallel-displaced and "sandwich" configuration with π–π stacking. These configurations are locally anisotropic and lead to the increasing of Kerr constant K. Analysis of the local structure was performed by calculating the cylindrical distribution function.

Key-Words: molecular dynamics simulation, comb polymer, local structure, pi-pi conjugation, phenyl rings

Received: June 9, 2023. Revised: November 19, 2023. Accepted: December 22, 2023. Published: February 2, 2024.

1 Introduction

Isotropic liquids have local (short-range) orientational order. Local orientational order exists due to the mutual orientation of densely packed anisometric molecules. The correlation length characterizing this order is small; it corresponds to two to three molecular sizes. The situation is different in the isotropic phase of liquid crystalline substances (LC). The correlation length in them increases many times when approaching the temperature T_c of the phase transition to the mesophase. This short-range orientational order in an isotropic melt of mesogens appears in macroscopic effects, which are called pre-transition. Despite this name, the effects are detected by the electrical birefringence method (Kerr effect) over a temperature range tens of degrees wide.

The structure of polymers is different from the structural organization of low molecular weight LC. Polymer melts are formed by long flexible macromolecules in a coil conformation. For this reason, obtaining the LC state in polymers previously seemed unlikely. The problem was solved when comb-shaped polymers were chosen as the basis for creating LC polymers. The roles of side groups were played by liquid crystal molecules. At the initial stage of their work, chemists attached mesogenic molecules directly to the main polymer chain. Mesophase did not arise in such polymers. Then the idea was born to attach mesogenic molecules to the chain through flexible spacers such as aliphatic chains. In this case, the side groups acquire relative independence from the chain and the ability to self-organize. This is how liquid crystalline polymers appeared, [1]. Inside the medium of disordered polymer coils, there is a subsystem formed by mutually ordered combs – providers of orientational order.

Studies of the isotropic phase of comb-shaped LC polymers have shown that their equilibrium electro-optical properties are well described by the Landau–de Gennes theory [2], [3]. In this, they are similar to low molecular weight LC [4], [5]. This suggests that the presence of polymer chains does not manifest itself noticeably in the short-range order in the mesogenic side group subsystem.

The results of these works drew our attention to the need to study polymers with the direct addition of anisotropic side groups to the chain. It is obvious that in their melts the short-range order and the macroscopic effects associated with it will be different.

Atactic polystyrene, in which phenyl rings are bonded to the main polymer chain, was chosen as a model for such a comb polymer, despite this is not LC. The phenyl rings make the main contribution to short-range order and local anisotropy. The electro-optical properties of melts of four fractions of styrene and polystyrene oligomers were studied earlier [6]. It turned out that for fractions with the highest degree of polymerization, the Kerr constant K does not decrease with increasing temperature, but, on the contrary, increases at temperatures above 120 °C. The observed effect may be associated with the liquid–liquid transition (ll-transition). It was observed in the equilibrium and dynamic properties of polymers, including polystyrene [7], [8]. The transition is explained by the fact that upon heating and reaching the ll transition temperature, the cooperativity of the movement

of the monomer units of the chain decreases; instead of segmental movement, the monomer unit becomes the main kinetic unit.

The increase in K may be due to the mutual ordering of the optically and dielectrically anisotropic phenyl rings included in the polystyrene monomer unit. The molecular dynamics method was used to simulate liquid benzene as an analog of the phenyl rings of polystyrene [6]. The configurations of the adjacent rings have been determined. Calculations have shown that at low temperatures, neighboring rings are predominantly in a mutual T-configuration, which has the lowest local anisotropy. Consequently, the increase in local anisotropy should occur due to an increase in the contributions of the sandwich configuration and the planar configuration.

2 Objects and Methods of Investigation

2.1 Objects and Simulation Details

In the present work, the molecular dynamics method [9] was used to simulate the liquid state of three substances: ethylbenzene (EB) as a monomer, pentastyrene (polystyrene-5, PS-5, strictly speaking, it is an oligomer), and polystyrene-25 (PS-25) as polymers consisted of 5 or 25 monomer units which are similar to EB. The purpose of the simulation was to determine the possibility of the ordering of phenyl rings in the substances in the isotropic phase.

Each molecule of polymer PS-5 or PS-25 was generated as an atactic isomer from monomer units which are conventionally called left (L) and right (D) with the use of a random number generator. In general, for polystyrene the meaning of L and D enantiomers is conditional, but two adjusting units form two types of dyads which are distinguishable from each other: the pair of the same units (either LL or DD) form *meso* (m) dyad, the pair of the different units (either LD or DL) form *racemic* (r) dyad. The number of L and D units and their sequences in PS-5 and PS-25 is in consistence with Bernoulli statistic [10], [11], [12] with probabilities $P(m) = P(r) = 0.5$ (Table 1). This is a reasonable model of industrially synthesized atactic polystyrene [13], [14], [15]. Examples of three molecules of PS-25 are shown in Fig.1.

All-atoms model was chosen. Parameters of intermolecular atom-atom interactions for carbon and hydrogen atoms were taken from the OPLS-AA [16] force field. All molecules are considered as flexible. Intramolecular interactions included bond angle bending, torsional (dihedral angle) rotations, and intramolecular Lennard-Jones and Coulombic pairwise interaction [17]. To speed-up simulation, the bond lengths were fixed by the SHAKE algorithm [18]. Verlet leap-frog algorithm [19] was used with a time step of 1 fs. Periodic boundary conditions with the Ewald method [20], [21] for the accounting of long-range electrostatic interactions were applied. The computer program AKMD was used.

Table 1. Chain statistics for generated atactic PS-5 and PS-25 molecules. Statistical weights of indistinguishable sequences of m and r dyads are summed. Data for the sequences up to pentads are presented.

Dyads sequence	Statistical weight of dyads (%) PS-5	PS-25	Bernoulli low
m	50.3	49.5	50
r	49.7	50.5	50
mm	25.6	24.2	25
mr, rm	48.8	50.4	50
rr	25.6	25.4	25
mmm	13.2	11.7	12.5
mmr, rmm	25.2	24.9	25
rrm, mrr	24.7	25.0	25
rmr	11.2	12.7	12.5
rrr	13.6	12.8	12.5
mrm	12.2	12.9	12.5
$mmmm$	6.6	5.4	6.25
$mmmr$, $rmmm$	13.1	12.4	12.5
$mmrr$, $rrmm$	12.7	11.8	12.5
$mmrm$, $mrmm$	11.8	13.5	12.5
$mrrm$	6.8	6.2	6.25
$mrrr$, $rrrm$	13.4	12.5	12.5
$mrmr$, $rmrm$	12.5	12.4	12.5
$rrmr$, $rmrr$	9.9	12.9	12.5
$rrrr$	6.9	6.5	6.25
$rmmr$	6.5	6.3	6.25

All the systems contained about an equal number of monomer units (3550–3555 units) combined in different numbers of molecules, which leads to similar cell sizes during simulation (Table 2).

Each molecule of PS-5 and PS-25 was generated in all-trans conformation as shown in Fig.1. In the first stage of simulation (annealing) every molecule was equilibrated *in vacuo* at a temperature of 175 °C during 0.5 ns. During this time, the energy of the molecules decreased, and they left all-trans conformation. After the equilibration, molecules were placed in the simulation cell. The orientation of molecules was random; centers of mass were placed in a regular network. The initial size of the simulation box was chosen big enough in order the molecules do not touch each other. The simulation box was slowly compressed in the *NVT* ensemble at $t = 175$ °C until the total energy of the system (potential plus kinetic) reached its minimum.

After the equilibration, the systems were simulated in an *NpT* ensemble [22] at pressure of 1 atm

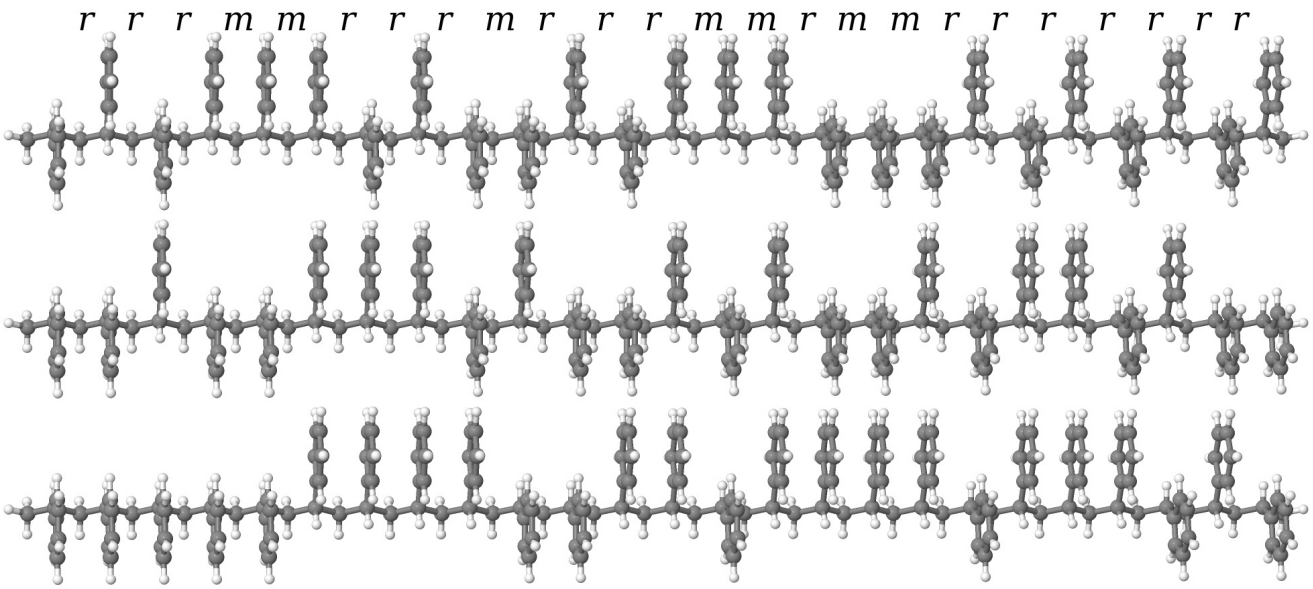

Fig. 1: Examples of three molecules of atactic PS-25 generated in all-trans conformation. Meso (m) and racemic (r) dyads are superscribed for the upper molecule

Table 2. Simulated systems and their parameters. Fluctuations of density and cell size in the *NpT* ensemble during simulation are shown. Molecular mass is calculated by accounting natural abundance of isotopes as it is recommended in the OPLS-AA force field.

Species	Number of molecules in a cell	Molecular mass, g mol^{-1}	Temperature, °C	Density, g cm^{-3}	Cell size, Å
EB	3554	106.2	25	0.864 ± 0.002	89.84 ± 0.05
PS-5	711	536.8	25	1.005 ± 0.001	85.75 ± 0.04
			175	0.926 ± 0.003	88.11 ± 0.08
PS-25	142	2619.8	25	1.002 ± 0.002	85.06 ± 0.04
			175	0.969 ± 0.002	86.04 ± 0.06

Table 3. Calculated diffusion coefficients.

Species	Temperature, °C	diffusion coefficients, m^2 s^{-1}
EB	25	$1.4 \cdot 10^{-9}$
PS-5	25	$1.1 \cdot 10^{-12}$
	175	$7.8 \cdot 10^{-11}$
PS-25	25	$9.5 \cdot 10^{-13}$
	175	$1.6 \cdot 10^{-12}$

and temperature of 175 °C during 25.5 ns; than trajectories were stored for 140.0 ns; than temperature was slowly changed to 25 °C and the systems were equilibrated for 30.0 ns; finally, trajectories were stored for 200.0 ns.

EB was simulated at 25 °C. Equilibration time was 2.4 ns; trajectories were stored for 4.7 ns. Diffusion coefficient of $1.4 \cdot 10^{-9}$ m^2/s (Table 3) and mean displacement of EB molecules from their initial positions during the analyzed period (54.7 Å) proved that the simulation time was enough to obtain averaged structural and dynamical parameters of EB molecules.

2.2 Cylindrical Distribution Function

The local structure of the substances around phenyl rings was analyzed in terms of cylindrical distribution function (CDF). The CDF is a kind of particle-particle distribution function $g_2^{\mathrm{AB}}(Z, R)$. It shows the distribution of particle B in the local frame of particle A. Both particles may be either a "real" particle (carbon or hydrogen atom) or "virtual" particle as, for example, the center of mass of carbon atoms of phenyl rings. Widely used radial distribution function (RDF) $g_2^{\mathrm{AB}}(R)$ is another kind of these functions. In contrast to one-dimensional isotropic RDF, the CDF is a two-dimensional function. This distribution shows the positions of particle B in the local

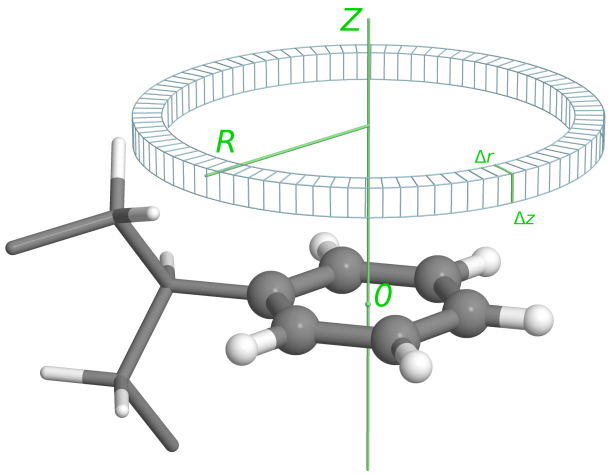

Fig. 2: On the definition of cylindrical distribution function (CDF) $g_2^{\mathrm{AB}}(Z,R)$. Atoms of a phenyl ring are shown in the ball-and-sticks model, part of the main chain of the polymer is shown with sticks in the left part of the figure. The center of mass of the carbon atoms of the ring is the origin O, Z axis coincides with the C_6 axis of symmetry of the ring. Explanation of the used values of height Δz and thickness Δr of cylindrical segments seen in the text

cylindrical frame of particle A. Originally, CDF was developed for the investigation of the local structure of nematic liquid crystals which molecules have got rotation axis of symmetry and recently were adapted to toluene (methylbenzene) [23]. In this work, the function was applied to the investigation of the local structure of phenyl rings of side-chain polymers and ethylbenzene (as monomer unit of the polymers).

In the present work, the "virtual particles A" are the phenyl rings of polystyrene or ethylbenzene molecules. The local cylindrical frame (Z,R) connected to the carbon atoms of the rings: six-fold symmetry axis (C_6) of a phenyl ring is taken as Z-axis, the origin O is in the center of mass of carbon atoms. This definition is shown in Fig.2. Coordinates Z and R of particle B are calculated in this frame. To calculate the distribution function, the space is separated into cylindrical segments of height Δz and thickness Δr. In this work, the values of height Δz and thickness Δr were chosen as 0.1 Å. Both coordinates, Z and R, are stepped with this value of 0.1 Å. Number of particles B n_{B} calculated inside each cylindrical segment. This corresponds to the calculation of a two-dimensional histogram. The distribution function is a normalized histogram according to the formula:

$$g_2^{\mathrm{AB}}(Z,R) = \frac{n_{\mathrm{B}}(Z,R,\Delta z,\Delta r)}{V_{\mathrm{segment}}(Z,R,\Delta z,\Delta r)} \Big/ \frac{N_{\mathrm{B}}}{V}$$

where n_{B} is the average number of particles B in the cylindrical segment $V_{\mathrm{segment}}(Z,R,\Delta z,\Delta r)$. The normalization coefficient is $\frac{N_{\mathrm{B}}}{V}$, where N_{B} is the total number of particles B in the simulation cell, and V is the volume of the cell. During a simulation, the number n_{B} is averaged for all the phenyl rings (particles A) of all the molecules (ensemble averaging) on each step of the trajectory (time averaging). The value of $g_2^{\mathrm{AB}}(Z,R) = 1$ corresponds to the mean density of the particles B in the segment (assuming they are equally distributed in the space). The value $g_2^{\mathrm{AB}}(Z,R) = 0$ near particle A shows so-called "excluded volume" of particle A. Excess of unity ($g_2^{\mathrm{AB}}(Z,R) > 1$) shows the position of solvation shell of the particle A by the particles B.

To picture the CDF, a two-dimensional plot of square pixels of size 0.1×0.1 Å^2 is performed as the gray-scale map. The medium gray pixel shows the value $g_2^{\mathrm{AB}}(Z,R) = 1$, the white pixel shows $g_2^{\mathrm{AB}}(Z,R) = 0$, black pixel corresponds to the value of 2 or more. Axis Z is plotted vertically, axis R is duplicated from right to left. As a result, the symmetric map is been shown.

3 Results and Discussion

CDFs of centers of mass of phenyl rings (as "virtual particles B") were calculated for three systems at 25 °C. They are presented in Fig.3. Excess of the density of particles B under and below center of the ring A is at the distance of 4.4–5.1 Å from the plane of ring A. Such distance between centers of rings allows to ring B turn perpendicular to ring A as schematically shown in Fig.3a. This corresponds to the T-configuration of adjacent rings [24].This result is similar to that obtained for benzene molecules in liquid phase [6]. Liquid benzene as well as ethylbenzene do not show local anisotropy.

Compared to the CDF of EB, in the CDF of polymeric PS-5, new regions of high probability of the neighboring rings appear diagonally left and right of the central ring (one of them is marked with a circle in Fig.3b). Such position of the center of ring B corresponds to the parallel-displaced configuration (possibly, tilted) of two adjacent rings. The scheme is included in the figure. Such a configuration is anisotropic.

Further, in CDF of PS-25 new high-density regions directly under and below the central ring at a distance of 3.5–4.1 Å exist. These positions of the centers of mass of ring B correspond to the "sandwich" configuration of two rings. Also, this configuration assumes π–π conjugation of aromatic rings. The parallel orientation of phenyl rings shows their local anisotropic ordering. The scheme is included in the Fig.3c.

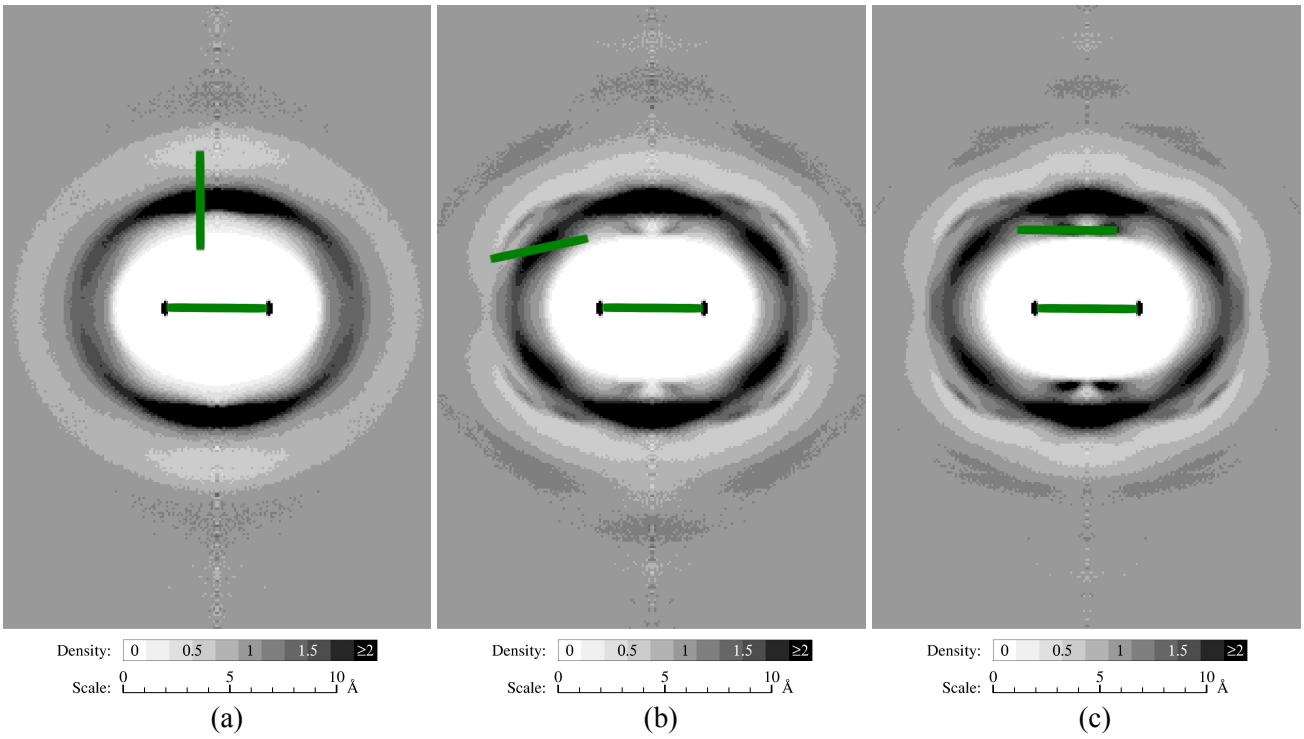

Fig. 3: Cylindrical distribution functions (CDFs) of centers of mass of phenyl rings as virtual "particles" B: (a) EB, (b) PS-5, (c) PS-25 at 25 °C. Inside the excluded volume of the central ring (virtual "particle" A), the distribution of hydrogen atoms of the central ring is shown as reference points (black). Green lines schematically show the most probable positions and orientations of two phenyl rings. The length of the green line corresponds to the distance H–H in the para position. In the system of EB, the only possible orientations of the rings are T-shaped (a), in the PS-5 system new parallel-displaced positions are added to the T-shaped (b), and in the PS-25 system other new positions of sandwich-type added with respect to PS-5 (c)

At higher temperatures of 175 °C additional high-density regions become less populated (Fig.4), but still exist.

These results are following the experimental data obtained earlier in the work [6]. The Kerr constant $K = 3.3 \cdot 10^{-12}$ (cm/300 V)^2 of PS-5 has the lowest average value among the measured polystyrene samples (PS-5, PS-25, PS-45, and PS-88, the two latest are not simulated in this work) at temperature 20 °C, and it is close to the constant K of benzene ($K = 2.1 \cdot 10^{-12}$ (cm/300 V)^2) and toluene ($K = 3.9 \cdot 10^{-12}$ (cm/300 V)^2) [6]. So, the local orientational order of phenyl rings in PS-5 and benzene molecules are comparable to each other. The fraction of phenyl rings in the T-configuration for both substances is sufficient to maintain the value of K at a low level because of this configuration is isotropic.

The formation of a coil in PS-25 leads to the restriction of the freedom of orientational mobility of the phenyl rings due to steric effects. As a result, the number of rings n_B in T-configuration decreases in favor of π–π conjugated configurations: "sandwich" and parallel-displaced. The decreasing of n_B leads to a decrease of both the area of T-configuration and the value of $g_2^{\mathrm{AB}}(Z, R)$, which is shown in Fig.3 and Fig.4. Therefore, the local anisotropy in polymer PS-25 increases, and the average value K becomes 1.5 times greater than K of the PS-5. Temperature dependence of K for both PS-5 and PS-25 has the classic form $K \propto (1/T)$ [6].

4 Conclusion

In this work, the cylindrical distribution function (CDF) $g_2^{\mathrm{AB}}(Z, R)$ was adapted to analyze the mutual positions and orientation of phenyl rings in the polystyrene PS-5 and PS-25. Molecules were generated and simulated as natural atactic polymers. All-atom model of flexible molecules was used. This model better describes local structure of polymeric molecules than united atoms and coarse grain models.

The modeling results and previously obtained experimental data allow us to make assumptions about the molecular mechanisms causing changes in short-range order (local structure) in polystyrene. Among them:

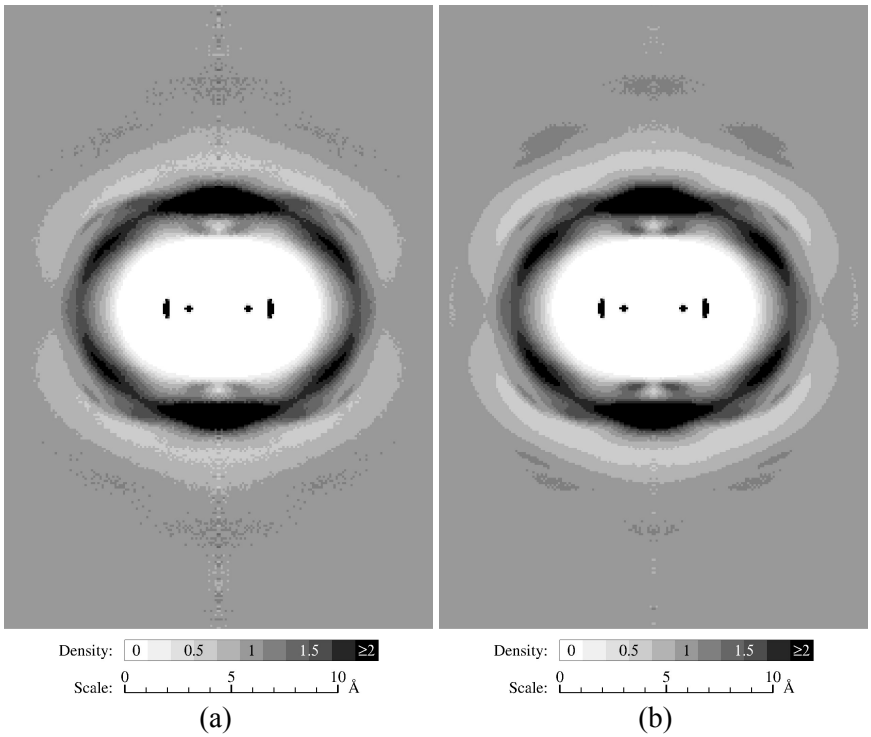

Fig. 4: Cylindrical distribution functions (CDFs) of centers of mass of phenyl rings as virtual "particles" B: (a) PS-5 and (b) PS-25 at 175 °C

1. strong influence of the length of the main chain on the orientation of phenyl rings;
2. an increase in the freedom of rotation of monomer units around single bonds of the main chain and an increase in the micro-Brownian motion of the units (an increase in kinetic flexibility) of the chain as a result of the liquid-liquid transition with increasing temperature;
3. the T-configuration is predominant in the ethylbenzene, PS-5, and PS-25;
4. the increase of the length of the polymeric chain leads to the decreasing probability of isotropic T-configuration and the increase of anisotropic "sandwich" configuration and parallel-displaced configuration of phenyl rings.

The future investigation will touch on unusual temperature behavior Kerr constant of PS-45 and PS-88 in the polystyrene melt.

Acknowledgment:
We sincerely thank A. E. Fedorov for his great technical assistance in preparing the published material.

References:

[1] V. Shibaev, Liquid Crystalline Polymers, in *Reference Module in Materials Science and Materials Engineering*, Elsevier, 2016, pp. 1-46.

[2] M. Eich, K. Ullrich, J. H. Wendorff, and H. Ringsdorf, Pretransitional phenomena in the isotropic melt of a mesogenic side chain polymer, *Polymer*, Vol.25, No.9, 1984, pp. 1271-1276.

[3] Th. Fuhrmann, M. Hosse, I. Lieker, J. Rubner, A. Stracke, and J. H. Wendorff, Frustrated liquid crystalline side group polymers for optical storage, *Liquid Cryst.*, Vol.26, No.5, 1999, pp. 779-786.

[4] J. Prost and J. R. Lalanne, Laser-Induced Optical Kerr Effect and the Dynamics of Orientational Order in the Isotropic Phase of a Nematogen, *Phys. Rev. A*, Vol.8, No.4, 1973, pp. 2090-2093.

[5] R. Yamamoto, S. Ishihara, S. Hayakawa, and K. Morimoto, The Kerr constants and relaxation times in the isotropic phase of nematic homologous series, *Phys. Lett. A*, Vol.69, No.4, 1978, pp. 276-278.

[6] S. G. Polushin, V. B. Rogozhin, G. E. Polushina, and A. V. Komolkin, Nanostructuring Polystyrene in a Melt,

Nanobiotechnology Reports, Vol.17, No.1, 2022, pp. 93-97.

[7] C. A. Glandt, H. K. Toh, J. K. Gillham, and R. F. Boyer, Effect of dispersity on the $T_{||}$ ($>T_g$) transition in polystyrene, *J. Appl. Polym. Science*, Vol.20, No.5, 1976, pp. 1277-1288.

[8] R. F. Boyer, Pressure dependence of secondary transitions in amorphous polymers. 1. $T_{||}$ for polystyrene, poly(vinyl acetate), and polyisobutylene, *Macromolecules*, Vol.14, No.2, 1981, pp. 376-385.

[9] M. P. Allen and D. J. Tildesley, *Computer Simulation of Liquids*, Oxford University Press, 2017.

[10] G. Moad and D. Solomon, *The Chemistry of Radical Polymerization*, Elsevier, 2005.

[11] M. Kobayashi, Section 2 - Structure of gels, characterization techniques, in *Gels Handbook*, Academic Press, 2001, pp. 172-412.

[12] F. Bovey, *High-Resolution NMR of Macromolecules*, Elsevier, 2012.

[13] C. Ayyagari, D. Bedrov, and G. D. Smith, Structure of Atactic Polystyrene: A Molecular Dynamics Simulation Study, *Macromolecules*, Vol.33, No.16, 2000, pp. 6194-6199.

[14] K. Matsuzaki, T. Uryu, K. Osada, and T. Kawamura, Stereoregularity of polystyrene-β,β-d_2, *Journal of Polymer Science: Polymer Chemistry Edition*, Vol.12, No.12, 1974, pp. 2873-2879.

[15] K. Matsuzaki, T. Uryu, T. Seki, K. Osada, and T. Kawamura, Stereoregularity of polystyrene and mechanism of polymerization, *Die Makromolekulare Chemie*, Vol.176, No.10, 1975, pp. 3051-3064.

[16] W. L. Jorgensen, D. S. Maxwell, and J. Tirado-Rives, Development and Testing of the OPLS All-Atom Force Field on Conformational Energetics and Properties of Organic Liquids, *J. Am. Chem. Soc.*, Vol.118, No.45, 1996, pp. 11225-11236.

[17] M. Chalaris, A. Koufou, K. Kravari, Dipole Moment of A-agents series via Molecular Dynamics Simulations, *Molecular Sciences and Applications*, Vol.3, 2023, pp. 1-4.

[18] J.-P. Ryckaert, G. Ciccotti, and H. J. C. Berendsen, Numerical integration of the cartesian equations of motion of a system with constraints: molecular dynamics of n-alkanes, *J. Comput. Phys.*, Vol.23, No.3, 1977, pp. 327-341.

[19] L. Verlet, Computer "Experiments" on Classical Fluids. I. Thermodynamical Properties of Lennard-Jones Molecules, *Phys. Rev.*, Vol.159, No.1, 1967, pp. 98-103.

[20] P. P. Ewald, Die Berechnung optischer und elektrostatischer Gitterpotentiale, *Ann. Phys.-Berlin*, Vol.369, No.3, 1921, pp. 253-287.

[21] S. W. de Leeuw, J. W. Perram, and E. R. Smith, Simulation of electrostatic systems in periodic boundary conditions. I. Lattice sums and dielectric constants, *Proc. R. Soc. A – Math. Phys.*, Vol.373, No.1752, 1980, pp. 27-56.

[22] S. Melchionna, G. Ciccotti, and B. L. Holian, Hoover *NPT* dynamics for systems varying in shape and size, *Molecular Physics*, Vol.78, No.3, 1993, pp. 533-544.

[23] V. Y. Bazaikin, A. V. Komolkin, D. A. Markelov, Journal of Molecular Liquids 383, 122188 (2023).

[24] S. E. Wheeler and J. W. G. Bloom, Toward a More Complete Understanding of Noncovalent Interactions Involving Aromatic Rings, *J. Phys. Chem. A*, Vol.118, No.32, 2014, pp. 6133-6147.

Contribution of Individual Authors to the Creation of a Scientific Article (Ghostwriting Policy)

The authors equally contributed in the present research, at all stages from the formulation of the problem to the final findings and solution.

Sources of Funding for Research Presented in a Scientific Article or Scientific Article Itself

No funding was received for conducting this study.

Conflicts of Interest

The authors have no conflicts of interest to declare that are relevant to the content of this article.